Transactions of the SMiRT 27
Yokohama, Japan, March 3-8, 2024
Division II

Effect of Element Size on Fracture Analysis by Damage Mechanics Models Considering the Effect of Strain Rate

Kenji Yashirodai[1], Motoki Nakane[2]

[1] Senior Researcher, Hitachi, Ltd., Hitachi, Ibaraki, Japan. (kenji.yashirodai.du@hitachi.com)
[2] Chief Engineer, Hitachi-GE Nuclear Energy, Ltd., Hitachi, Ibaraki, Japan.

ABSTRACT

Fracture analysis using a damage mechanics model is applied for evaluating the limit load and fracture behavior of nuclear power plant equipment. The Gurson-Tvergaard-Needleman (GTN) model, which is a damage mechanics model that incorporates the nucleation and growth of voids into the constitutive law, is applied to ductile fracture analysis. However, failure analysis using a damage mechanics model is affected by element size, and since fractures tend to have a large plastic deformation locally, the influence of the strain rate cannot be disregarded. In this study, the effects of element dimensions and strain rate on fracture analysis with the GTN model were investigated through compression and tensile tests of smooth bar and notched bar specimens of low alloy steel for SQV2A pressure vessels. Based on the compression test results, the material parameters for the GTN model were determined by matching the deformation behavior of the tensile test of the smooth bar specimen. Within the scope examined in this study, it was confirmed that the effect of element size and strain rate on deformation behavior was minor. On the other hand, the material parameter f_F, which defines element failure, showed different tendencies depending on whether or not strain rate effect was used. In addition, by determining the material parameter f_F based on the element division number for diameter, it was confirmed that the strain that initiates a sudden load drop in the notched bar specimen can be conservatively evaluated.

INTRODUCTION

Fracture analysis using a damage mechanics model, such as the Gurson-Tvergaard-Needleman (GTN) model proposed by Needleman et al. and Tvergaard et al. (1984), is applied for evaluating the limit load and fracture behavior of nuclear power plant equipment. The GTN model, which is a damage mechanics model that incorporates the nucleation and growth of voids into the constitutive law, is applied to ductile fracture analysis. However, to apply the GTN model to the failure analysis of real structures, the effect of element size must be considered, as reported by Kiran et al. (2014) and Watanabe et al. (2014). Moreover, since fractures tend to have a large plastic deformation locally, the influence of the strain rate cannot be disregarded. In this study, the effect of element size and strain rate on fracture analysis by the GTN model was investigated.

EVALUATION METHOD

Gurson-Tvergaard-Needleman (GTN) model

The GTN model is a type of damage mechanics model that can simply express ductile fracture. The yield function in the GTN model is defined by

$$\Phi = \left(\frac{\sigma_{eq}}{\sigma_y}\right)^2 + 2q_1 f^* \cosh\left(-\frac{3q_2}{2}\frac{\sigma_h}{\sigma_y}\right) - \left(1 + q_3 f^{*2}\right) = 0, \quad (1)$$

where σ_{eq} is the macroscopic Mises yield stress that includes voids, σ_h is the hydrostatic stress, and σ_y is the yield stress in a completely dense condition (no voids exist). q_1, q_2, and q_3 are yield function parameters introduced as correction factors by Tvergaard and Needleman, and are generally defined as $q_3 = {q_1}^2$. f^* models the rapid loss of stress-bearing capacity due to void coalescence, and is defined as a function of the void volume fraction f.

The amount of change in the void volume fraction f in the material is given by the sum of the amount of change due to void growth $\dot{f}_{gr}$ and void nucleation $\dot{f}_{nucl}$. The void nucleation is controlled by strain, and is expressed by

$$\dot{f}_{nucl} = \dot{\varepsilon}_{eq}^{pl} \frac{f_N}{s_N\sqrt{2\pi}} exp\left[-\frac{1}{2}\left(\frac{\varepsilon_{eq}^{pl}-\varepsilon_N}{s_N}\right)^2\right], \quad (2)$$

where ε_N and s_N respectively denote the average value and standard deviation of the strain at which voids occur, which is given as a normal distribution. f_N is the volume fraction of generated voids, and voids are generated only in cases under tensile stress.

In this study, the material parameters of the GTN model were determined by utilizing the stress-strain relationship obtained in a compression test, which theoretically does not generate voids, as base data and fitting it to the results of a tensile test on a smooth round bar specimen. The determination of each material parameter was carried out in two stages. The first stage involved studying the material parameters q_1, q_2, $q_3\,(={q_1}^2)$, ε_N, s_N, f_N, and f_0 regarding the generation and growth of voids that are independent of element size effect. The second stage involved studying the material parameters fF and fc, which are related to element fracture. The initial void volume function f_0 was determined from the content of S and Mn, with reference to a report that assumed it was generated by the precipitation of MnS (Franklin, 1969).

Experimental method

In this study, low alloy steel for SQV2A pressure vessels was used as the test material. Table 1 shows the chemical composition of SQV2A, and Fig. 1 shows the shape of the specimens used in the tensile test.

The compressive test was conducted to obtain the stress-strain relationship in a dense condition, which serves as the base data for the GTN model, and to study the strain rate dependence of the yield surface. To consider the influence of strain rate due to elastic follow-up at the notch bottom of the round notched bar specimen, crosshead displacement speeds of 0.0288, 0.288, and 6.0 mm/min were used. The crosshead displacement speed of 0.288 mm/min in the compressive test was set separately based on the results of elastic-plastic FEA to match the strain rate with the crosshead displacement speed of 0.5 mm/min in the tensile test of the smooth bar specimens.

The tensile test using smooth bar specimens was conducted to determine the material parameters of the GTN model and evaluate the strain rate dependence of the yield surface. The tensile test using notched bar specimens was conducted using two types of similar shapes with different dimensions to evaluate the influence of stress triaxiality and dimensional effect on fracture analysis. The crosshead displacement speeds of 0.5 and 5.0 mm/min were used for the tensile test of the smooth bar specimen, and a speed of 0.5 mm/min was used for the tensile test of the notched bar specimen.

Table 1 Chemical composition of low alloy steel for SQV2A pressure vessels. (wt. %)

	C	Si	Mn	P	S	Ni	Mo	Fe
Measured	0.17	0.25	1.43	0.002	0.000	0.65	0.55	Bal.

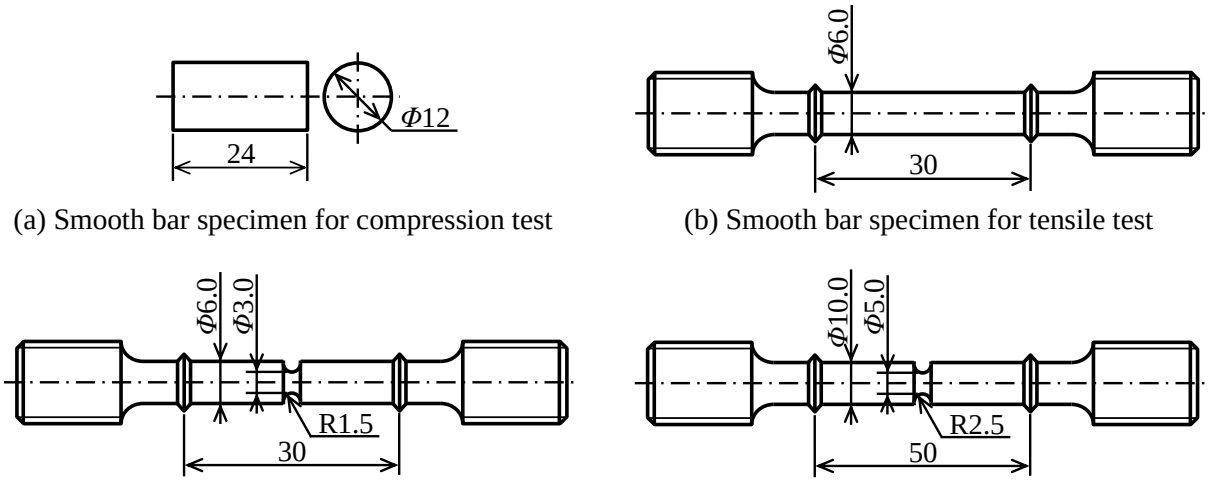

(a) Smooth bar specimen for compression test

(b) Smooth bar specimen for tensile test

(c) Notched bar specimen (R = 1.5) for tensile test

(d) Notched bar specimen (R = 2.5) for tensile test

Fig. 1 Shapes and dimensions of specimens for tensile test. (unit: mm)

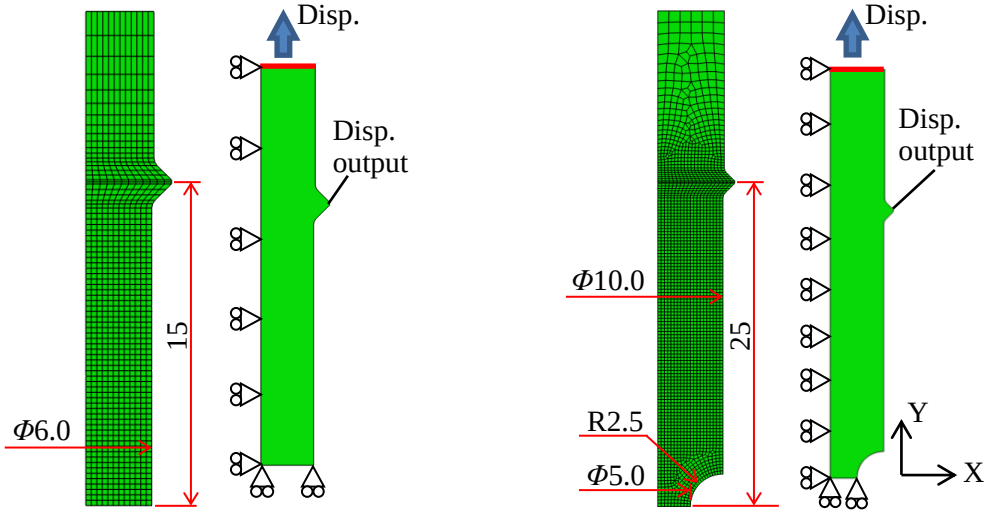

(a) Smooth bar specimen

(b) Notched bar specimen (R = 2.5)

Fig. 2 FEA models and boundary conditions for round bar specimens.

FEA simulation methods

In this study, finite element analysis (FEA) was utilized to determine each material parameter of the GTN model. Elastic-plastic analysis was performed using a smooth bar specimen model for tensile tests, and each material parameter of the GTN model was determined by matching the deformation behavior obtained by FEA with the deformation behavior of the tensile test result.

Figure 2 shows an analysis model of the tensile specimens used for FEA and representative examples of boundary conditions. The FEA models were half-models from the viewpoint of specimen symmetry, and were modelled with axisymmetric elements. To consider the influence on the stress and strain distribution of the shape discontinuity around the extensometer mounting part, the FEA model includes the shape around the extensometer mounting part. In addition, to evaluate the influence of element dimensions, four types of FEA models with element dimensions of 0.5–0.05 mm were prepared.

FEA was executed using the finite element analysis code Abaqus Version 2018. The explicit method was utilized to perform fracture analysis using the GTN model. The element type used for FEA was the four-node primary axisymmetric element with reduced integral CAX4R. The elastic-plastic stress–strain relationship was defined by the isotropic hardening law using data that approximated the true stress σ_t–true plastic strain ε_{tp} relationship obtained from compression test results. Young's modulus E was 207 GPa, and Poisson's ratio ν was 0.3.

RESULTS AND DISCUSSION

Results of compression and tensile tests

The results of the compression and tensile tests are summarized in Table 2 In the compression test, no significant barrel-shaped deformation or buckling deformation was observed, so it was judged that an effective stress-strain relationship was obtained.

Elastic-plastic property data for FEA was prepared based on the test results of the compression test. In the compression test results of SQV2A, since it changes continuously at the end of the yield point, the true stress σ_t- true plastic strain ε_t^{pl} relationship in the transition region was defined by

$$\sigma_t = 161\log_{10}\frac{1}{\sqrt{1+\left(100\varepsilon_t^{pl}\right)^3}} + 439.3\,. \tag{3}$$

The correction for the strain rate dependence of the stress-strain relationship was determined based on the test results of the compression specimen. Since the true strain when the maximum stress occurred in the tensile test of the smooth bar specimen was approximately 0.12, the relationship between stress and strain rate at a true strain of 0.12 was compared. The correction for the strain rate dependence of the stress-strain relationship was determined based on the test results of the compression specimen. Since the true strain when the maximum stress occurred in the tensile test of the smooth bar specimen was approximately 0.12, the relationship between stress and strain rate at a true strain of 0.12 was compared. Figure 3 shows the stress-strain rate relationship obtained in the compression and tensile tests. Referring to the estimation equation for the strain rate dependence of tensile strength defined in WES 2808 (2017), the correction for the strain rate dependence of yield stress was defined by the strain rate correction coefficient α, as

Table 2 Summary of compression and tensile test results.

TP type	TP no.	Dimension		Tensile test				
		Diameter (mm)	Gauge length (mm)	Yield stress (MPa)	UTS (MPa)	Elon-gation (%)	Reduction of area (%)	Disp. speed at crosshead (mm/min)
Smooth bar	SB-1	6.02	30.0	473	586	24	75	0.5
	SB-2	6.01	30.0	472	594	25	76	5.0
Notched bar (R = 2.5 mm)	NB1-1	5.04	50.0	–	773	3	63	0.5
	NB1-2	4.99	50.0	–	761	3	62	0.05
Notched bar (R = 1.5 mm)	NB2-1	3.02	30.0	–	774	3	61	0.5
Smooth bar (Comp.)	CTP-1	12.02	24.03	443	–	–	–	0.288
	CTP-2	12.03	24.01	447	–	–	–	0.288
	CTP-3	12.03	24.02	452	–	–	–	6.0
	CTP-4	12.02	24.01	436	–	–	–	0.0288

$$\alpha = \frac{\sigma_t}{\sigma_{t0}} = \exp\left[8 \times 10^{-4} \cdot \left(\frac{\sigma_0}{E}\right)^{-1.5} \left\{\frac{1}{\ln\left(10^8/\dot{\varepsilon}_t^{pl}\right)} - \frac{1}{\ln\left(10^8/\dot{\varepsilon}_{t0}^{pl}\right)}\right\}\right], \quad (4)$$

where $\dot{\varepsilon}_{t0}^{pl}$ is the reference true strain rate, and σ_{t0} is the true stress at the reference true strain rate. In this study, after fitting four items of compression test data, the parameters σ_{t0} and $\dot{\varepsilon}_{t0}^{pl}$ in Eq. (4) were set to 747.3 MPa and 1.166×10^{-2}/min, respectively.

Equation (4) is based on the tensile strength σ_B defined by nominal stress, but in this study, it was utilized as a reference to define the strain rate dependence of yield surface. As shown in Fig. 4, it was confirmed that the strain rate dependence of the compression test result can be approximated by Eq. (4). The strain rate correction of the yield surface in the FEA was performed by outputting the yield stress at an arbitrary strain rate σ_y (= $\alpha\sigma_{y0}$) after obtaining the correction factor α based on Eq. (4) utilizing the strain rate at each step of FEA.

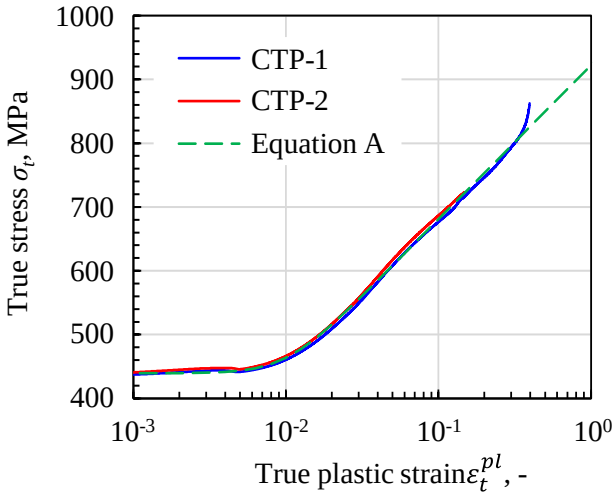

Fig. 3 True stress σ_t–true plastic strain ε_t^{pl} curves obtained by compression test.

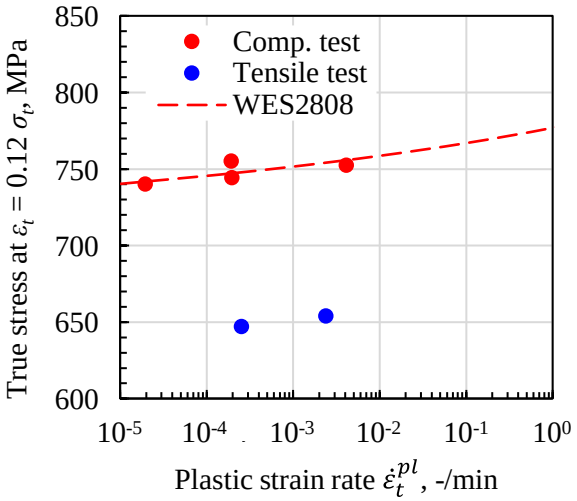

Fig. 4 Strain rate dependence of stress at ε_t = 0.12.

Determination of material parameters based on compression test results

As the first step for determining the material parameters of the GTN model, Table 3 shows a comparison of each material parameter obtained after examining the material parameters (excluding f_F, f_c, which are related to element destruction), and Fig. 5 shows a comparison with the tensile test results of the smooth round bar specimen. Here, an FEA model with a minimum element size of 0.25 mm was utilized to examine each material parameter.

In the comparison between the tensile test results of the smooth specimen shown in Fig. 5(a) and the FEA results, the load drop behavior after the maximum stress occurred could not be completely reproduced in conditions that do not include the effect of strain rate, and the amount of load drop tended to be overestimated. The reason for this behavior is that priority was given to matching the maximum stress, and it was thought that the load drop was overestimated because the void volume fraction *f* was too large to reproduce the deformation behavior after the maximum stress. On the other hand, the stress drop behavior after the maximum stress occurred could be completely reproduced in conditions that include the strain rate effect. The is presumably thanks to the expansion of the yield surface due to an increase in strain rate following the necking of the test piece after the maximum stress occurred.

For the deformation behavior of the notched bar specimens shown in Fig. 5(b) and (c), the deformation behavior could be accurately reproduced regardless of whether or not the strain rate effect was included. Specifically, FEA using the GTN model, which included the strain rate effect, estimated the stress slightly lower.

The above examination demonstrates that the reproducibility of the deformation behavior of the smooth bar specimen and the notched bar specimen could be evaluated more appropriately by including the strain rate effect from the viewpoint of deformation reproducibility.

Table 3 Material parameters for GTN model and Shear modified GTN model.

	f_0	q_1	q_2	ε_N	S_N	f_N
GTN w/o strain rate	0.0	1.5	0.2	0.000	0.135	0.100
GTN w/ strain rate	0.0	1.5	0.3	0.000	0.135	0.130

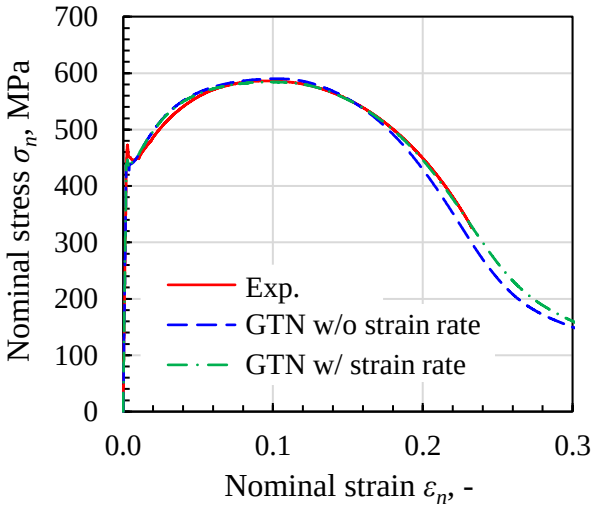

(a) Smooth bar specimen

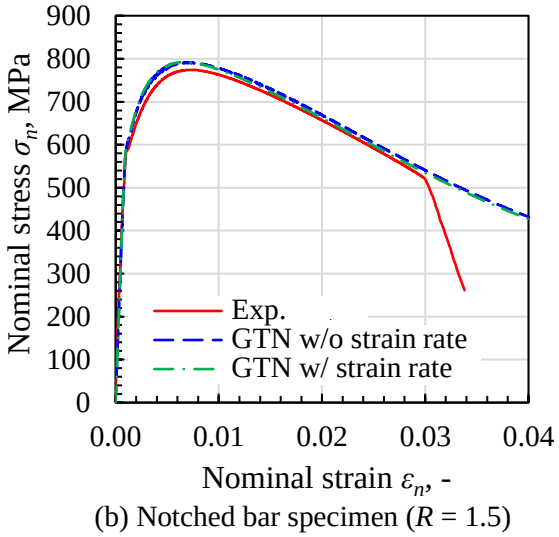

(b) Notched bar specimen (R = 1.5)

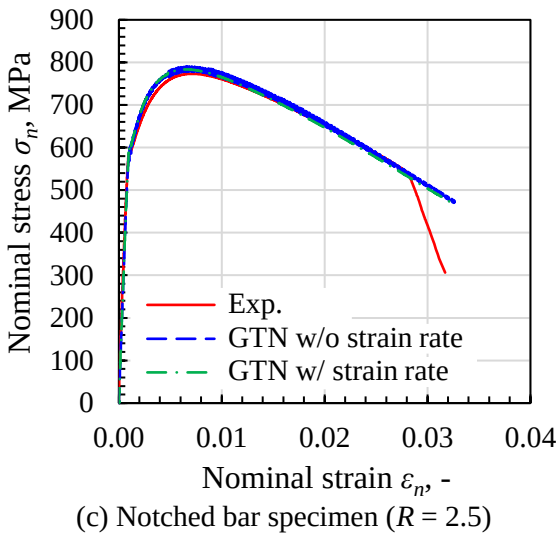

(c) Notched bar specimen (R = 2.5)

Fig. 5 Example of nominal stress σ_n–nominal strain ε_n relations obtained by fitting results of material parameters for GTN model.

Effect of specimen shape and element size

As the second stage of investigating the material parameters of the GTN model, the results of examining the material parameters f_F, f_c related to the destruction of elements of the GTN model are presented in this section.

To determine the material parameter f_F for element failure, FEA models of smooth bar and notched bar specimens prepared with minimum element sizes of 0.5, 0.25, 0.1, and 0.05 mm were used. FEA of a smooth bar specimen and two types of notched bar specimens was performed using a GTN model that did not include the material parameter f_F for element failure obtained in the previous section. The void volume fraction f at the nominal strain when the rapid load drop occurs in each tensile test was set to the material parameter f_F for element failure. Here, f_c was presumed to be equal to f_F.

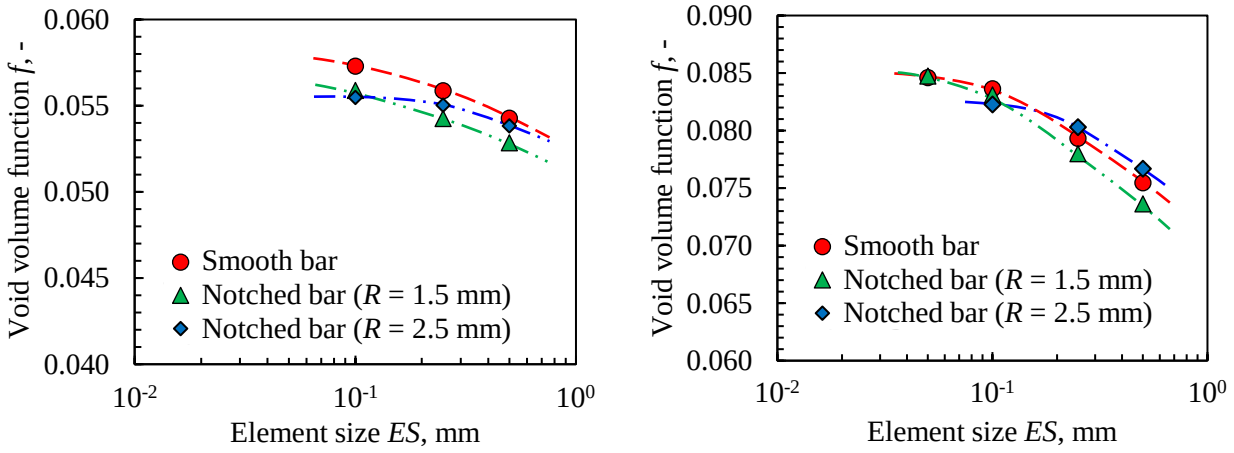

(a) Element size

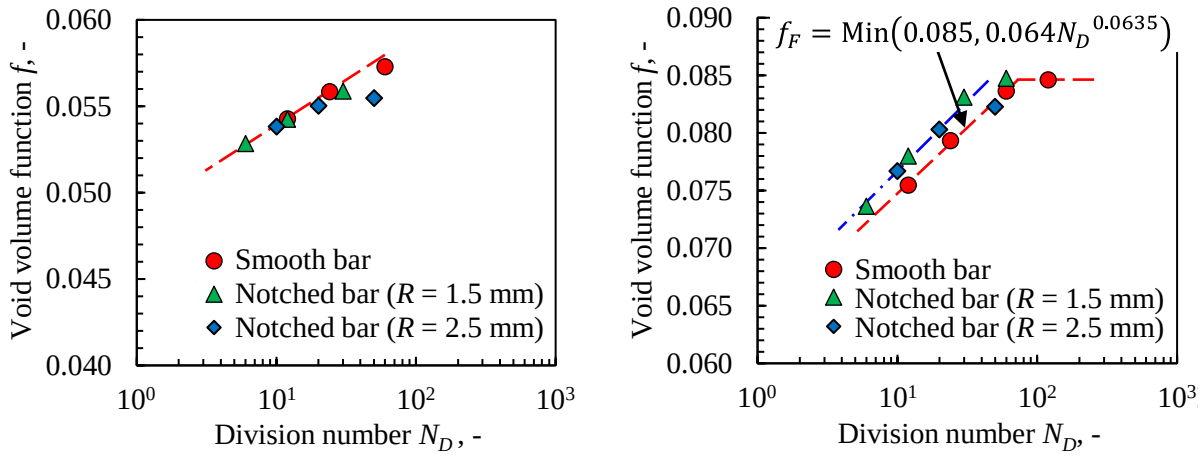

(b) Division number for diameter

Fig. 6 Relationship between void volume function f and division number for diameter N_D.

Fig. 6 shows the relationship between the determined material parameter f_F and the element size ES and division number for diameter N_D. In Fig. 6(a), which compares the element size with the material parameter f_F for the element failure of each specimen, the variation of f_F obtained between each

specimen was large, and a difference was also observed between the two types of notched specimens with similar shapes. In particular, regardless of whether or not the strain rate effect was included, the notched bar specimen with notch radius R = 2.5 mm tended to converge at the material parameter f_F, which is smaller than the other specimens, as the element size decreases. This tendency indicates that the convergence value of f_F depends on the size and shape of the specimen. In addition, when the material parameter f_F was determined using the element size standard based on the tensile test results of the smooth bar specimen, the fracture ductility of the notched specimen tended to be overestimated.

On the other hand, the comparison results based on the division number for diameter in Fig. 6(b) show that, under conditions that do not include the strain rate effect, the material parameter f_F of the smooth bar specimen and two types of notched bar specimen can be arranged in the same straight line, except for one condition of the notched bar specimen where R = 2.5 mm. This trend was roughly the same as the report by Yashirodai et al. (2022).

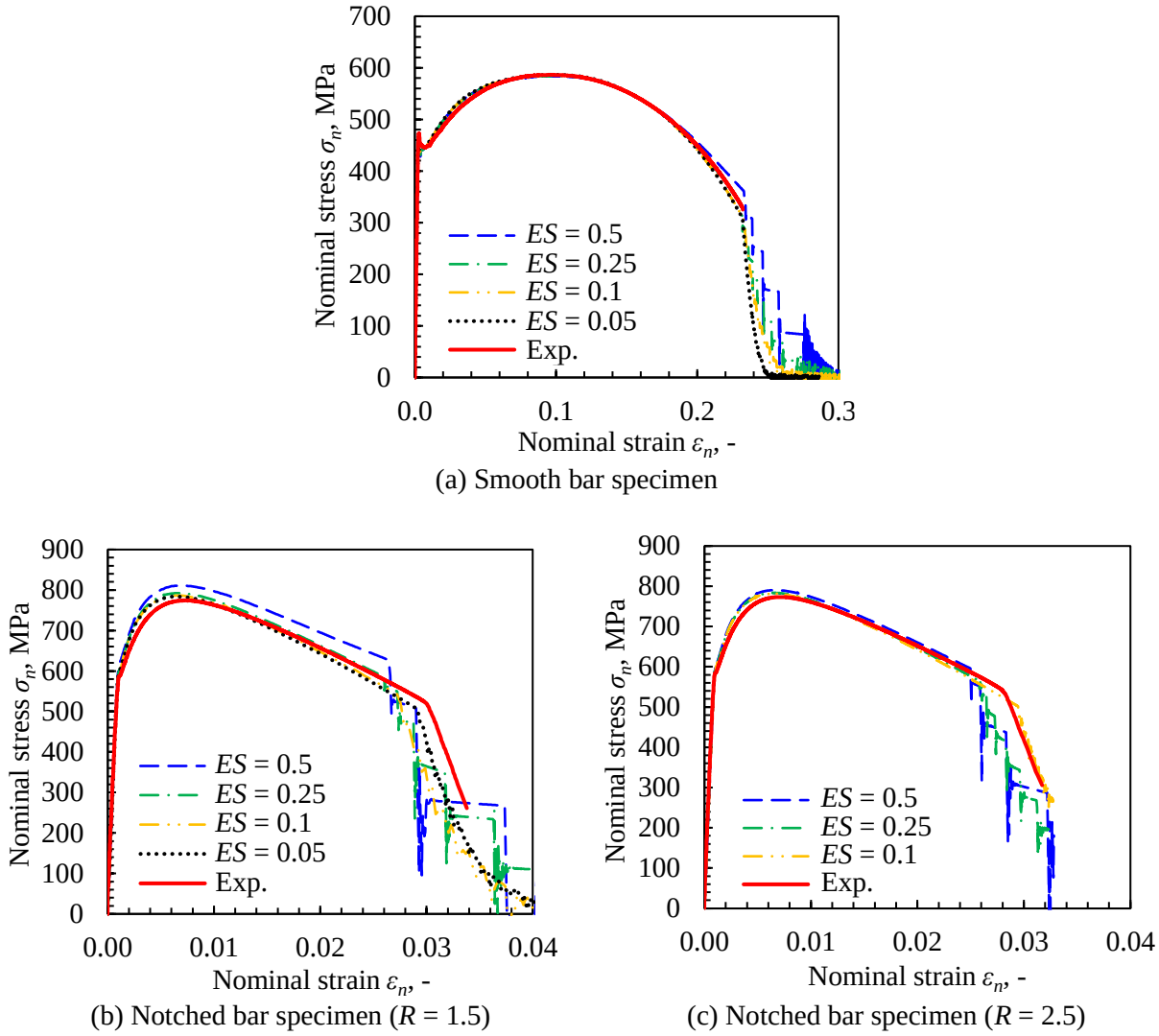

(a) Smooth bar specimen

(b) Notched bar specimen (R = 1.5)

(c) Notched bar specimen (R = 2.5)

Fig. 7 Comparison between tensile test results and fracture analysis results calculated by GTN model with strain rate effect and several element sizes of model for smooth bar and notched bar specimens.

The comparison results based on the division number for diameter show that, under conditions including the strain rate effect, the material parameter f_F of the two types of notched bar specimens tended to be larger than that of the smooth bar specimen when the division number was 60 or less. However, since these results can be organized in a straight line featuring the same slope with respect to the division number, there is a similar tendency for the division number. Therefore, in the region of the division number, the same tendency is shown, at least in notched bar specimens of a similar shape, so the material parameter f_F presumably corresponds to the distribution of stress and strain. In addition, it can be estimated that the phenomenon in which the material parameter f_F tends to converge at about 0.085 under conditions with a large division number of elements is due to the fact that the number of element divisions is sufficiently large for the distribution of stress and strain. However, there is a possibility that it converges to a lower value under the condition of R = 2.5 mm for the notched bar specimen. An examination of this possibility is left to future work.

Based on the above tendency, Fig. 7 shows the failure analysis results including the strain rate effect using the material parameter f_F determined based on the division number using the results of the smooth bar specimen. Here, the material parameter f_F was defined by

$$f_F = \mathrm{Min}\left(0.085,\ 0.064{N_D}^{0.0635}\right), \tag{5}$$

as described in Fig. 6(b) ii).

As shown in Fig. 7, which compares the FEA results and tensile test results of the smooth bar specimen and annular notched bar specimens, it was confirmed that the deformation behavior of each specimen can be roughly reproduced, although the nominal strain at the start of the failure of the notched bar specimens was evaluated to be somewhat small.

CONCLUSION

In this study, the effects of element dimensions and strain rate on fracture analysis with the GTN model were investigated for compression and tensile tests of smooth bar and notched bar specimens of low alloy steel for SQV2A pressure vessels. Based on the compression test results, the material parameters for the GTN model were determined by matching the deformation behavior of the tensile test of the smooth bar specimen. Within the scope examined in this study, it was confirmed that the effect of the element size and strain rate on deformation behavior was minor. On the other hand, the material parameter f_F, which defines element failure, showed different tendencies depending on whether or not strain rate effect was applied. In addition, by determining the material parameter f_F based on the element division number for the diameter of the smooth bar specimen, it was confirmed that the strain that initiates a sudden load drop in the notched bar specimen can be conservatively evaluated.

REFERENCES

A. Needleman and V. Tvergaard, “An analysis of ductile rupture in notched bars,” *J. Mech. Phys. Solids*, vol. 32, pp. 2–15, 1984.

V. Tvergaard and A. Needleman, “Analysis of the Cup-cone Fracture in a Round Tensile Bar,” *Acta. Metall*., vol. 32, pp. 157–169, 1984.

R. Kiran and K. Khandelwal, “Gurson model parameters for ductile fracture simulation in ASTM A992 steels,” *Fatigue & Fracture of Engineering Materials & Structures*, vol. 37, issue 2, pp. 171–183, 2014.

D. Watanabe, Y. Chuman, T. Kamisasanuki, and K. Hojo, “Experimental study of Gurson model parameter determination method for ductile fracture,” *Proc. of the Mat. and Mech. Conf. 2014*, OS0815, 2014.

K. Yashirodai and M. Nakane, “Effect of Element Size on Fracture Analysis Results by using Damage Mechanics Models,” *Proc. of the Mat. and Mech. Conf. 2022*, OS0112, 2022.

The Japan Welding Engineering Society, “WES 2808:2017 Method of assessing brittle fracture in steel weldments subjected to large cyclic and dynamic strain,” 2017.

A. G. Franklin, “Comparison between a quantitative microscope and chemical methods for assessment of non-metallic inclusions,” *J. Iron Steel Inst.*, vol. 207, pp. 181–186, 1969.